Wireless Personal Communications manuscript No.
(will be inserted by the editor)

The Asymmetric Golden Code for Fast Decoding on Time-Varying Channels

Mohanned O. Sinnokrot · John R. Barry · Vijay K. Madisetti

Received: date / Accepted: date

Abstract The golden code is a full-rate full-diversity space-time code for the two-input two-output channel with good performance but high decoding complexity. The overlaid Alamouti codes were recently proposed as an alternative; in exchange for a slight performance penalty, they have lower decoding complexity on quasistatic channels with QAM alphabets. However, the complexity advantage of the overlaid codes vanishes for time-varying channels. This paper proposes the *asymmetric golden code*, a novel full-rate and full-diversity space-time code for the two-input two-output channel that offers reduced-complexity decoding on both quasistatic and time-varying channels.

Keywords Golden code · Nonvanishing determinant · Transmit diversity

1 Introduction

Communication systems having two transmit and two receive antennas are of great practical importance, in part because power and size constraints prevent many devices from having more than two antennas. Similarly, the desire for high spectral efficiency motivates space-time codes with high rate. Therefore, the class of full-rate space-time codes for two-input two-output channels is especially important and has been incorporated into the 802.16e standard [1].

Early space-time codes were designed either to increase the diversity gain [2][3], or to increase the multiplexing gain [4]. Zheng and Tse [5] showed that there is a continuous tradeoff between the achievable diversity and multiplexing gains. Yao and Wornell [6] proved that a sufficient condition for achieving the diversity-multiplexing tradeoff is that the code possess a nonvanishing determinant [7]. The golden code, proposed independently in [7] and [8], has a nonvanishing determinant and in terms of the SNR required to achieve a target error probability, it performs better than all previously reported full-rate codes with two transmit antennas.

Mohanned O. Sinnokrot · John R. Barry · Vijay K. Madisetti
School of Electrical and Computer Engineering, Georgia Institute of Technology, Atlanta, GA 30339, USA.
E-mail: {sinnokrot,barry,vkm}@ece.gatech.edu

A rate-two space-time code is said to be *fast decodable* when the worst-case complexity of a maximum-likelihood (ML) decoder for a quasistatic channel is $\mathcal{O}(q^{2.5})$, where q is the alphabet size [9]. A class of fast-decodable 2×2 space-time codes was recently proposed as alternatives to the golden code [10]-[12]; we call the codes of [10]-[12] overlaid Alamouti codes because they are based on a layering of two Alamouti space-time block codes. See [13] for a survey of the overlaid Alamouti codes. For the special case of QAM alphabets, the golden code itself is fast decodable on both quasistatic and time-varying channels [9], and the overlaid Alamouti codes have worst-case decoding complexity that is even smaller, namely $\mathcal{O}(q^2)$.

The overlaid Alamouti codes lose their fast-decodable property when the channel varies with time, a common occurrence in wireless applications with high mobility. In this paper we propose a full-rate space-time code with a nonvanishing determinant that is fast decodable in both quasistatic and rapidly time-varying channels. In particular, we propose the *asymmetric golden code*, which is constructed over QAM alphabets, and in which one layer of the golden code is scaled with respect to the other. We prove that its worst-case decoding complexity is $\mathcal{O}(q^{2.5})$, regardless of whether the channel is time varying. For the special case of quasistatic fading, we prove that it has a decoding complexity of $\mathcal{O}(q^2)$, the same as the overlaid Alamouti codes. Furthermore, we present an efficient implementation of a fast ML decoder for quasistatic channels. The asymmetric golden code has the lowest decoding complexity among previously proposed codes and maintains its low decoding complexity on both quasistatic and time-varying channels.

The remainder of the paper is organized as follows. In Section 2.2, we present the system model and review background material. In Section 3 we present the proposed asymmetric golden code and prove its fast decoding properties in quasistatic and time-varying channels. In Section 4, we introduce a fast ML decoder with low average complexity for quasistatic fading. In Section 5 we present numerical results, and in Section 6 we draw conclusions.

2 Background

2.1 System Model

We consider space-time coding for a system with two transmit antennas and two receive antennas transmitting four complex information symbols over two symbol periods. The transmitted codeword can be expressed as a 2×2 matrix:

$$\mathbf{C} = \begin{bmatrix} c_1[1] & c_2[1] \\ c_1[2] & c_2[2] \end{bmatrix}, \tag{1}$$

where $c_m[k]$ denotes the symbol transmitted from antenna $m \in \{1, 2\}$ at time $k \in \{1, 2\}$. The received signal $y_n[k]$ at receive antenna $n \in \{1, 2\}$ at time k is given by:

$$y_n[k] = \sum_{m=1}^{2} c_m[k] h_{m,n}[k] + w_n[k], \tag{2}$$

where $w_n[k]$ is the complex additive-white Gaussian noise at receive antenna n at time k, and $h_{m,n}[k]$ is the channel coefficient between the m-th transmit antenna and n-th

receive antenna at time k. For quasistatic fading, $h_{m,n}[k] = h_{m,n}$ is independent of time k.

The maximum spatial diversity order for the two-input two-output channel is the product of the number of transmit and number of receive antennas, namely four. The following two design criteria for space-time codes over quasistatic fading channels were derived in [3]:

- *Rank Criterion*: To achieve fourth order diversity, the difference matrix $\Delta\mathbf{C} = \mathbf{C} - \tilde{\mathbf{C}}$ must have rank two for any pair of distinct codewords $\mathbf{C}$ and $\tilde{\mathbf{C}}$.
- *Determinant Criterion*: To further optimize performance, a code with full diversity should be chosen to maximize the coding gain. For 2×2 square matrices, the coding gain expression simplifies to:

$$\Gamma = \min_{\mathbf{C} \neq \tilde{\mathbf{C}}} \left| \det(\mathbf{C} - \tilde{\mathbf{C}}) \right|. \tag{3}$$

Similar criteria were proposed for rapid-fading channels in [3].

2.2 Unified Framework for the Encoding of High-Rate Space-Time Codes for the Two-Input Two-Output Channel

We present a common framework for comparing the golden code and the overlaid Alamouti codes in a unified way. In Section 3 we will use this framework to describe the asymmetric golden code. All of these codes transmit four complex information symbols $\{x_1, x_2, x_3, x_4\}$ from two transmit antennas in two signaling intervals, and they may all be viewed as the sum of a pair of rate-one codes. In particular, all may be described by the following 2×2 space-time code:

$$\mathbf{C}(\mathbf{x}) = \mathbf{C}_1(\mathbf{a}) + \mathbf{\Phi}_L \mathbf{C}_1(\hat{\mathbf{b}}) \mathbf{\Phi}_R, \tag{4}$$

where:

- $\mathbf{x} = [x_1, x_2, x_3, x_4]^\top$, $\mathbf{a} = [x_1, x_2]^\top$, $\mathbf{b} = [x_3, x_4]^\top$, $\hat{\mathbf{b}} = \mathbf{\Phi}_P \mathbf{b}$;
- $\mathbf{\Phi}_P$ is a unitary precoding matrix;
- $\mathbf{C}_1(\cdot)$ is a rate-one encoder for symbol pairs $\mathbf{a}$ or $\hat{\mathbf{b}}$;
- $\mathbf{\Phi}_L$ and $\mathbf{\Phi}_R$ are 2×2 matrices that multiply $\mathbf{C}_1(\hat{\mathbf{b}})$ on the left and right, respectively.

The four parameters $\mathbf{C}_1(\cdot)$, $\mathbf{\Phi}_L$, $\mathbf{\Phi}_L$, and $\mathbf{\Phi}_L$ are chosen to ensure full diversity, maximize the coding gain and reduce decoding complexity.

One possibility for $\mathbf{C}_1(\cdot)$ is the diagonal algebraic space-time code of [14], defined by:

$$\mathbf{C}_{DAST}(a_1, a_2) = \begin{bmatrix} u_1 & 0 \\ 0 & u_2 \end{bmatrix}, \tag{5}$$

where

$$\begin{bmatrix} u_1 \\ u_2 \end{bmatrix} = \mathbf{G} \begin{bmatrix} a_1 \\ a_2 \end{bmatrix}, \; \mathbf{G} = \begin{bmatrix} c & s \\ -s & c \end{bmatrix}, \tag{6}$$

and

$$c = \cos(\theta), s = \sin(\theta), \theta = \frac{1}{2}\tan^{-1}(2), \text{ and } \phi = e^{j\pi/4}. \tag{7}$$

Another possibility is the Alamouti code:

$$\mathbf{C}_{Alamouti}(a_1, a_2) = \frac{1}{\sqrt{2}} \begin{bmatrix} a_1 & a_2 \\ -a_2^* & a_1^* \end{bmatrix}, \tag{8}$$

where the constant $1/\sqrt{2}$ ensures that the total transmit energy is identical to the energy of the underlying alphabet.

The golden code is a special case of (4) with:

$$\mathbf{C}_1 = \mathbf{C}_{DAST}, \mathbf{\Phi}_P = \mathbf{I}_2, \mathbf{\Phi}_L = e^{i\pi/4}\mathbf{I}_2, \mathbf{\Phi}_R = \begin{bmatrix} 0 & 1 \\ 1 & 0 \end{bmatrix}. \tag{9}$$

The overlaid Alamouti codes of [10][11] are a special case of (4) with:

$$\mathbf{C}_1 = \mathbf{C}_{Alamouti}, \mathbf{\Phi}_P = \begin{bmatrix} \phi_1 & \phi_2 \\ -\phi_2^* & \phi_1^* \end{bmatrix}, \mathbf{\Phi}_L = \begin{bmatrix} 1 & 0 \\ 0 & -1 \end{bmatrix}, \mathbf{\Phi}_R = \mathbf{I}_2, \tag{10}$$

where

$$\phi_1 = \frac{1}{\sqrt{7}}(1+i) \text{ and } \phi_2 = \frac{1}{\sqrt{7}}(1+2i). \tag{11}$$

Finally, the overlaid Alamouti code of [12] is also a special case of (4), with:

$$\mathbf{C}_1 = \mathbf{C}_{Alamouti}, \mathbf{\Phi}_P = \mathbf{I}_2, \mathbf{\Phi}_L = \frac{\alpha}{|\alpha|} \begin{bmatrix} 1 & 0 \\ 0 & -i \end{bmatrix}, \mathbf{\Phi}_R = \mathbf{I}_2, \tag{12}$$

where

$$\alpha = (1-\sqrt{7}) + i(1+\sqrt{7}). \tag{13}$$

The worst-case decoding complexity of the golden code is $\mathcal{O}(q^{2.5})$ in both quasistatic and time-varying fading for QAM alphabets [9]. The overlaid Alamouti codes with QAM are fast-decodable with worst-case decoding complexity of $\mathcal{O}(q^2)$ in quasistatic fading channels [13], but lose their fast decoding property on time-varying channels and have a worst-case complexity of $\mathcal{O}(q^3)$. We next present the asymmetric golden code, which has a worst-case decoding complexity of $\mathcal{O}(q^2)$ in quasistatic channels and $\mathcal{O}(q^{2.5})$ in time-varying channels, which is the lowest decoding complexity compared to previously reported rate-two space-time block codes for the two-input two-output channel.

3 The Asymmetric Golden Code

We propose a novel full-rate full-diversity space-time code for the two-input two-output channel: the *asymmetric golden code*. We first describe encoding, and then prove the fast decoding properties of the asymmetric golden code.

3.1 The Asymmetric Golden Code Encoder

We propose the asymmetric golden code, a special case of (4) with

$$\mathbf{C}_1 = \mathbf{C}_{\mathcal{K}}, \mathbf{\Phi}_P = \mathbf{I}_2, \mathbf{\Phi}_L = \mathcal{K}\mathbf{I}_2, \mathbf{\Phi}_R = \begin{bmatrix} 0 & 1 \\ 1 & 0 \end{bmatrix}, \tag{14}$$

where $\mathcal{K} \in (0,1)$ is an *asymmetry coefficient*, to be specified later. The factor $\mathcal{K}$ in $\mathbf{\Phi}_L$ ensures that the second layer will be scaled by $\mathcal{K}$ before being added to the first layer. The rate-one encoder $\mathbf{C}_{\mathcal{K}}$ in (14) is a modified version of the diagonal algebraic encoder in (5), defined by:

$$\mathbf{C}_{\mathcal{K}}(a_1, a_2) = \sqrt{\frac{2}{1+\mathcal{K}^2}} \begin{bmatrix} u_1 & 0 \\ 0 & u_2^* \end{bmatrix}, \tag{15}$$

where $[u_1, u_2]^\top$ is given by (6).

Comparing (15) to $\mathbf{C}_{DAST}$ of (5), we see two differences: the constant $\sqrt{\frac{2}{1+\mathcal{K}^2}}$, which ensures that the average transmit energy is equal to that of the underlying alphabet, and the conjugation of u_2. The latter makes $\mathbf{C}_{\mathcal{K}}$ different from $\mathbf{C}_{DAST}$ even when $\mathcal{K} = 1$. Let $\mathbf{a} = [x_1, x_2]^\top$ and $\mathbf{b} = [x_3, x_4]^\top$. Then, in terms of the original information symbols, the asymmetric golden code is given by

$$\mathbf{C} = \sqrt{\frac{2}{1+\mathcal{K}^2}} \left(\begin{bmatrix} \tilde{a}_1 & 0 \\ 0 & \tilde{a}_2^* \end{bmatrix} + \mathcal{K} \begin{bmatrix} 0 & \tilde{b}_1 \\ \tilde{b}_2^* & 0 \end{bmatrix} \right) \tag{16}$$

$$= \sqrt{\frac{2}{1+\mathcal{K}^2}} \begin{bmatrix} cx_1 + sx_2 & \mathcal{K}(cx_3 + sx_4) \\ \mathcal{K}(-sx_3^* + cx_4^*) & -sx_1^* + cx_2^* \end{bmatrix}, \tag{17}$$

where:

$$\tilde{\mathbf{a}} = \mathbf{G}\mathbf{a}, \quad \tilde{\mathbf{b}} = \mathbf{G}\mathbf{b}, \text{ and } \mathbf{G} = \begin{bmatrix} c & s \\ -s & c \end{bmatrix}, \tag{18}$$

and c, s, and ϕ are given by (7).

Theorem 1 *The asymmetry coefficient $\mathcal{K} \in (0,1)$ that maximizes the coding gain (3) for the space-time block code in (16) with QAM alphabet is $K = 1/\sqrt{3}$. The resulting coding gain is $1/\sqrt{20}$.*

Proof See Appendix A. □

We next describe the effective channel matrix induced by the asymmetric golden code. We then establish the key properties of this matrix, and describe a maximum-likelihood decoder that exploits the key properties to reduce complexity in rapid time-varying fading as well as quasistatic fading.

3.2 The Effective Channel Matrix and its Key Properties

Substituting the definition of the asymmetric golden code from (16) into (2), the vector of samples after conjugating the second and fourth samples received at a receiver with two antennas at the two time instances can be written as the output of an effective four-input four-output channel:

$$\mathbf{y} = \mathbf{H}\mathbf{x} + \mathbf{n}, \tag{19}$$

where $\mathbf{y} = [y_1[1], y_1^*[2], y_2[1], y_2^*[2]]^\top$ is the vector of received samples after conjugation, $\mathbf{x} = [x_1, x_2, x_3, x_4]^\top$ is the vector of information symbols, $n = [n_1[1], n_1^*[2], n_2[1], n_2^*[2]]^\top$ is the noise, and where $\mathbf{H} = \bar{\mathbf{H}}\mathbf{\Psi}$ is the *effective channel matrix*:

$$\mathbf{H} = \underbrace{\sqrt{\frac{3}{2}} \begin{bmatrix} h_{1,1}[1] & 0 & \mathcal{K}h_{2,1}[1] & 0 \\ 0 & h_{2,1}^*[2] & 0 & \mathcal{K}h_{1,1}^*[2] \\ h_{1,2}[1] & 0 & \mathcal{K}h_{2,2}[1] & 0 \\ 0 & h_{2,2}^*[2] & 0 & \mathcal{K}h_{1,2}^*[2] \end{bmatrix}}_{\bar{\mathbf{H}}} \underbrace{\begin{bmatrix} c & s & 0 & 0 \\ -s & c & 0 & 0 \\ 0 & 0 & c & s \\ 0 & 0 & -s & c \end{bmatrix}}_{\mathbf{\Psi}}. \tag{20}$$

The structure of the asymmetric golden code induces special properties in its effective channel matrix that we exploit to reduce decoding complexity. The following two lemmas relate these special properties to the orthogonal-triangular (QR) decomposition $\mathbf{H} = \mathbf{QR}$, which results from an application of the Gram-Schmidt procedure to the columns of $\mathbf{H} = [\mathbf{h}_1, \cdots, \mathbf{h}_4]$, where the columns of $\mathbf{Q} = [\mathbf{q}_1, \cdots, \mathbf{q}_4]$ are an orthonormal basis for the subspace spanned by $\mathbf{H}$, and $\mathbf{R}$ is upper triangular with nonnegative real diagonal elements, so that the entry of $\mathbf{R}$ in row i and column j is $r_{i,j} = \mathbf{q}_i^* \mathbf{h}_j$. We present the key properties for fast decoding on time-varying fading and quasistatic fading in the following two lemmas.

Lemma 1 (The Key Property in Time-Varying Fading) *The* $\mathbf{R}$ *matrix in a QR decomposition* $\mathbf{H} = \mathbf{QR}$ *of the effective channel (20) has the form*

$$\mathbf{R} = \begin{bmatrix} \mathbf{A} & \mathbf{B} \\ \mathbf{0} & \mathbf{D} \end{bmatrix}, \tag{21}$$

where both of the upper triangular matrices $\mathbf{A}$ *and* $\mathbf{D}$ *are entirely real.*

Proof The proof follows immediately from [9] (c.f. Appendix A), where $\bar{\mathbf{H}}$ and $\mathbf{\Psi}$ are given in (20). □

A few remarks:

- Both $\mathbf{A} = \begin{bmatrix} r_{1,1} & r_{1,2} \\ 0 & r_{2,2} \end{bmatrix}$ and $\mathbf{D} = \begin{bmatrix} r_{3,3} & r_{3,4} \\ 0 & r_{4,4} \end{bmatrix}$ are triangular by construction with real diagonal entries, so the key property is the fact that both $r_{1,2}$ and $r_{3,4}$ are real.
- To demonstrate that $r_{1,2} = \mathbf{h}_1^* \mathbf{h}_2 / \|\mathbf{h}_1\|$ is real, it is sufficient to show that the inner product between the first two columns is real, a fact which is easily verified by direct computation.
- The lemma applies regardless of whether the channel is quasistatic or time-varying. For the case of quasistatic fading, however, permuting the channel matrix prior to QR decomposition leads to an $\mathbf{R}$ matrix with $r_{1,2} = r_{3,4} = 0$. We next discuss the key property of this permuted effective channel matrix in quasistatic fading.

Let us introduce the permutation matrix $\mathbf{\Pi} = [\mathbf{e}_1, \mathbf{e}_4, \mathbf{e}_2, \mathbf{e}_3]$, where $\mathbf{e}_i$ is the i-th column of the 4×4 identity matrix, so that (19) can be written as:

$$\begin{aligned} \mathbf{y} &= \mathbf{H}\mathbf{\Pi}\mathbf{\Pi}^\top \mathbf{x} + \mathbf{n} \\ &= \mathbf{H}_{\mathit{\Pi}} \mathbf{x}_{\mathit{\Pi}} + \mathbf{n}, \end{aligned} \tag{22}$$

where $\mathbf{x}_{\mathit{\Pi}} = \mathbf{\Pi}^\top \mathbf{x} = [x_1, x_4, x_2, x_3]^\top$ and $\mathbf{H}_{\mathit{\Pi}} = \mathbf{H}\mathbf{\Pi} = \bar{\mathbf{H}}\mathbf{\Psi}\mathbf{\Pi}$ is the *permuted effective channel matrix* given by

$$\mathbf{H}_{\mathit{\Pi}} = \underbrace{\sqrt{\frac{3}{2}} \begin{bmatrix} h_{1,1}[1] & 0 & \mathcal{K}h_{2,1}[1] & 0 \\ 0 & h^*_{2,1}[2] & 0 & \mathcal{K}h^*_{1,1}[2] \\ h_{1,2}[1] & 0 & \mathcal{K}h_{2,2}[1] & 0 \\ 0 & h^*_{2,2}[2] & 0 & \mathcal{K}h^*_{1,2}[2] \end{bmatrix}}_{\bar{\mathbf{H}}} \underbrace{\begin{bmatrix} c & s & 0 & 0 \\ -s & c & 0 & 0 \\ 0 & 0 & c & s \\ 0 & 0 & -s & c \end{bmatrix}}_{\mathbf{\Psi}} \underbrace{\begin{bmatrix} 1 & 0 & 0 & 0 \\ 0 & 0 & 1 & 0 \\ 0 & 0 & 0 & 1 \\ 0 & 1 & 0 & 0 \end{bmatrix}}_{\mathbf{\Pi}}. \tag{23}$$

The following lemma presents the key property in quasistatic fading.

Lemma 2 (The Key Property in Quasistatic Fading) *The* $\mathbf{R}$ *matrix in a QR decomposition* $\mathbf{H}_{\mathit{\Pi}} = \mathbf{Q}\mathbf{R}$ *of the permuted effective channel (23) has the form*

$$\mathbf{R} = \begin{bmatrix} \mathbf{A} & \mathbf{B} \\ \mathbf{0} & \mathbf{D} \end{bmatrix}, \tag{24}$$

where both $\mathbf{A}$ *and* $\mathbf{D}$ *are real and diagonal.*

Proof See Appendix B. □

We also remark that by construction, both $\mathbf{A} = \begin{bmatrix} r_{1,1} & r_{1,2} \\ 0 & r_{2,2} \end{bmatrix}$ and $\mathbf{D} = \begin{bmatrix} r_{3,3} & r_{3,4} \\ 0 & r_{4,4} \end{bmatrix}$ are upper triangular with real diagonal entries, so the key property in quasistatic fading is essentially the fact that $r_{1,2} = r_{3,4} = 0$.

3.3 The Asymmetric Golden Code is Fast-Decodable

We start with the case of time-varying fading. We show how the key property of Lemma 2 enables fast decoding. If we define $\mathbf{z}_{12} = [z_1, z_2]^\top$ and $\mathbf{z}_{34} = [z_3, z_4]^\top$, where $\mathbf{z} = \mathbf{Q}^*\mathbf{y}$, then the ML decision minimizes the cost function

$$\begin{aligned} P(\mathbf{x}) &= \|\mathbf{y} - \mathbf{H}\mathbf{x}\|^2 = \|\mathbf{z} - \mathbf{R}\mathbf{x}\|^2 \\ &= \|\mathbf{z}_{12} - \mathbf{A}\mathbf{a} - \mathbf{B}\mathbf{b}\|^2 + \|\mathbf{z}_{34} - \mathbf{D}\mathbf{b}\|^2. \end{aligned} \tag{25}$$

The last equality follows from (24). Therefore, the ML decisions $\hat{\mathbf{a}}$ and $\hat{\mathbf{b}}$ can be found recursively using:

$$\hat{\mathbf{b}} = \arg \min_{\mathbf{b} \in \mathcal{A}^2} \{\|\mathbf{z}_{12} - \mathbf{A}\mathbf{a}_*(\mathbf{b}) - \mathbf{B}\mathbf{b}\|^2 + \|\mathbf{z}_{34} - \mathbf{D}\mathbf{b}\|^2\}, \tag{26}$$

$$\hat{\mathbf{a}} = \mathbf{a}_*(\hat{\mathbf{b}}), \tag{27}$$

where

$$\mathbf{a}_*(\mathbf{b}) = \arg \min_{\mathbf{a} \in \mathcal{A}^2} \{\|\mathbf{z}_{12} - \mathbf{A}\mathbf{a} - \mathbf{B}\mathbf{b}\|^2\}. \tag{28}$$

The function $\mathbf{a}_*(\hat{\mathbf{b}})$ in (28) can be viewed as producing the best $\mathbf{a}$ for a given $\mathbf{b}$. With this interpretation, the optimization in (26) can be viewed as that of finding the best $\mathbf{b}$ when $\mathbf{a}$ is optimized.

The optimization (28) is equivalent to ML detection for a channel $\mathbf{A}$ with an input of $\mathbf{a}$ and an output:

$$\mathbf{v} = \mathbf{z}_{12} - \mathbf{B}\mathbf{b}. \tag{29}$$

It can be solved by a sphere detector applied to a two-level tree. With two QAM inputs and without any constraints on $\mathbf{A}$, the worst-case complexity would be $\mathcal{O}(q)$. This is because for every candidate symbol x_2, the decoder decides on the corresponding symbol x_1 with a slicer whose complexity does not grow with the size of the alphabet[1]. But the golden code induces the special property that $\mathbf{A}$ is real, which enables us to determine the real components of $\mathbf{a}$ *independently* from its imaginary components in (28). Specifically, we may rewrite (28) as:[2]

$$\mathbf{a}_*(\mathbf{b}) = \arg \min_{\mathbf{a}\in\mathcal{A}^2} \{\|\mathbf{v}^R - \mathbf{A}\mathbf{a}^R\|^2 + \|\mathbf{v}^I - \mathbf{A}\mathbf{a}^I\|^2\} \tag{30}$$

$$= \arg \min_{\mathbf{a}^R\in(\mathcal{A}^R)^2} \{\|\mathbf{v}^R - \mathbf{A}\mathbf{a}^R\|^2\} + j\cdot \arg \min_{\mathbf{a}^I\in(\mathcal{A}^I)^2} \{\|\mathbf{v}^I - \mathbf{A}\mathbf{a}^I\|^2\}. \tag{31}$$

Thus, the optimization in (28) decomposes into the pair of independent optimizations of (31). Since each optimization in (31) is equivalent to ML detection for a real channel with two $\sqrt{q}$-PAM inputs, each has a worst-case complexity of $\mathcal{O}(\sqrt{q})$. Thus, the overall complexity of (31) is $\mathcal{O}(\sqrt{q})$. We thus arrive at the fast decodability theorem on time-varying channels.

Theorem 2 (The Asymmetric Golden Code is Fast-Decodable on Time-Varying Fading) *A maximum-likelihood decoder for the asymmetric golden code with a q-ary QAM alphabet can be implemented with a worst-case complexity of* $\mathcal{O}(q^{2.5})$ *on time-varying fading channel.*

Proof The ML decision can be found by stepping through each of the q^2 candidates for $\mathbf{b}$ as described in (26), and for each implement the $\mathcal{O}(\sqrt{q})$ optimization of (31). □

We next discuss the case of quasistatic fading and show how the key property in Lemma 2 can also be used to reduce the worst-case ML decoding complexity. We start by defining the intermediate variables $\mathbf{c} = [x_1, x_4]^\top$, $\mathbf{d} = [x_2, x_3]^\top$, $\mathbf{z}_{12} = [z_1, z_2]^\top$ and $\mathbf{z}_{34} = [z_3, z_4]^\top$, where $\mathbf{z} = \mathbf{Q}^*\mathbf{y}$. The ML decision minimizes the cost function

$$\begin{aligned} P(\mathbf{x}) &= \|\mathbf{y} - \mathbf{H}\mathbf{x}\|^2 = \|\mathbf{z} - \mathbf{R}\mathbf{x}\|^2 \\ &= \|\mathbf{z}_{12} - \mathbf{A}\mathbf{c} - \mathbf{B}\mathbf{d}\|^2 + \|\mathbf{z}_{34} - \mathbf{D}\mathbf{d}\|^2. \end{aligned} \tag{32}$$

The last equality follows from Lemma 2. Therefore, the ML decisions $\hat{\mathbf{c}}$ and $\hat{\mathbf{d}}$ can also be found recursively using:

$$\hat{\mathbf{d}} = \arg \min_{\mathbf{d}\in\mathcal{A}^2} \{\|\mathbf{z}_{12} - \mathbf{A}\mathbf{c}_*(\mathbf{d}) - \mathbf{B}\mathbf{d}\|^2 + \|\mathbf{z}_{34} - \mathbf{D}\mathbf{d}\|^2\}, \tag{33}$$

$$\hat{\mathbf{c}} = \mathbf{c}_*(\hat{\mathbf{d}}), \tag{34}$$

[1] A QAM slicer can be implemented as a pair of PAM slicers, with each requiring a single multiply, a single rounding operation, a single addition, and a single hard-limiting operation, none of which depends on q.

[2] Throughout the paper we use superscripts R and I to denote the real and imaginary components, respectively, so that $\mathbf{v}^R = \Re\{\mathbf{v}\}$ and $\mathbf{v}^I = \Im\{\mathbf{v}\}$.

where

$$\mathbf{c}_*(\mathbf{d}) = \arg\min_{\mathbf{c}\in\mathcal{A}^2}\{\|\mathbf{z}_{12} - \mathbf{A}\mathbf{c} - \mathbf{B}\mathbf{d}\|^2\}. \tag{35}$$

Similar to $\mathbf{a}_*(\hat{\mathbf{b}})$ in (28), the function $\mathbf{c}_*(\hat{\mathbf{d}})$ in (35) can be viewed as producing the best $\mathbf{c}$ for a given $\mathbf{d}$. With this interpretation, the optimization in (33) can be viewed as that of finding the best $\mathbf{d}$ when $\mathbf{c}$ is optimized.

The optimization (35) is equivalent to ML detection for a channel $\mathbf{A}$ with an input of $\mathbf{c}$ and an output:

$$\mathbf{v} = \mathbf{z}_{12} - \mathbf{B}\mathbf{d}. \tag{36}$$

Because the asymmetric golden code induces the special property that $\mathbf{A}$ is diagonal and real, we can determine the four components of $\mathbf{c}$ *independently* from each other. Specifically, we may rewrite (35) as:

$$\begin{aligned}\mathbf{c}_*(\mathbf{d}) &= \arg\min_{\mathbf{c}\in\mathcal{A}^2}\{\|\mathbf{v} - \mathbf{A}\mathbf{c}\|^2\}\\ &= \arg\min_{x_4^R\in(\mathcal{A}^R)}\{|v_2^R - r_{2,2}x_4^R|^2\} + i\cdot\arg\min_{x_4^I\in(\mathcal{A}^I)}\{|v_2^I - r_{2,2}x_4^I|^2\} +\\ &\quad \arg\min_{x_1^R\in(\mathcal{A}^R)}\{|v_1^R - r_{1,1}x_1^R|^2\} + i\cdot\arg\min_{x_1^I\in(\mathcal{A}^I)}\{|v_1^I - r_{1,1}x_1^I|^2\}.\end{aligned} \tag{37}$$

The optimization in (35) decomposes into four independent optimizations of (37). Each optimization in (37) can be implemented with a slicer. Hence, the overall complexity of (37) is $\mathcal{O}(1)$. We thus arrive at the fast decodability theorem on quasistatic channels.

Theorem 3 (The Asymmetric Golden Code is Fast-Decodable on Quasistatic Fading) *A maximum-likelihood decoder for the asymmetric golden code with q-ary QAM alphabet can be implemented with a worst-case complexity of* $\mathcal{O}(q^2)$.

Proof As described in (33), the ML decision can be found by stepping through each of the q^2 candidates for $\mathbf{d}$, and for each implement the $\mathcal{O}(1)$ optimization of (37). □

4 Fast ML Decoding with Low Average Decoding Complexity

The decoding strategy used to prove the fast-decodable theorems has a low worst-case complexity but a high average complexity. In this section we present an efficient implementations of an ML decoder for the asymmetric golden code in quasistatic fading. The proposed ML decoder has a low average complexity and a worst-case complexity of $\mathcal{O}(q^2)$. An efficient ML decoder of the golden code for time-varying channel was proposed in [9], with a worst-case complexity of $\mathcal{O}(q^{2.5})$. Importantly, the algorithm in [9] [cf. Fig. 2] can be used to the decode the asymmetric golden code in time-varying fading without any modification to the algorithm. The inputs to the decoding algorithm, which are the received vector and the effective channel matrix are given by (19) and (20), respectively. Therefore, we will only consider efficient ML decoding in quasistatic fading.

A conventional sphere decoder applied to the asymmetric golden code results in a four-level tree, with a different $x_i, i \in \{1,2,3,4\}$, associated with each level. We propose a *three-level* tree that associates x_3 with the first level, x_2 with the second level and $\mathbf{c} = [x_1, x_4]^\top$ with the third level, as illustrated in Figure 1. This new tree

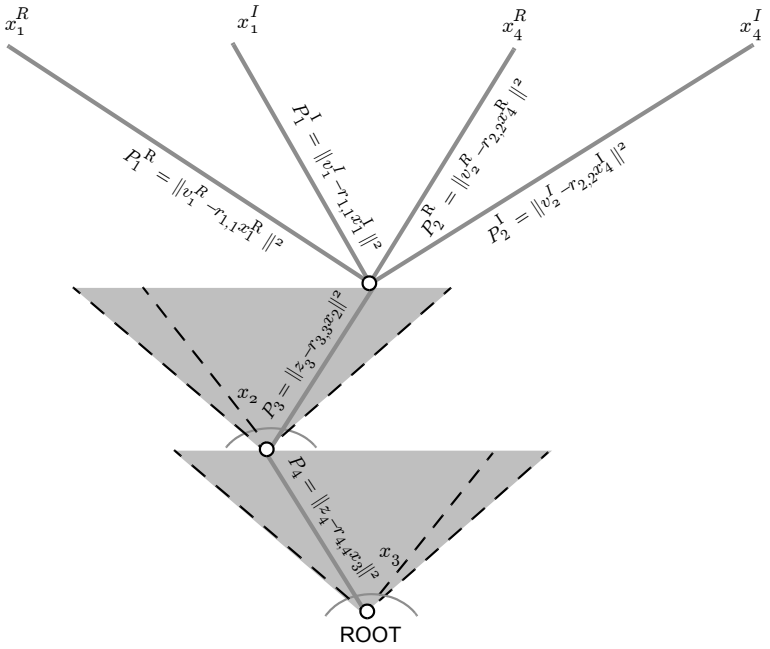

Fig. 1 The structure of the proposed detection tree and its branch metrics for the asymmetric golden code. The cost function for the leaf node is the sum of the branch metrics, $P(\mathbf{x}) = P_1^R + P_1^I + P_2^R + P_2^I + P_3 + P_4$.

is a direct result of the fact that $\mathbf{A}$ and $\mathbf{D}$ are real and diagonal (Lemma 2), which allows us to rewrite the ML cost function from (32) as

$$P(\mathbf{x}) = \overbrace{\underbrace{\|v_1^R - r_{1,1}x_1^R\|^2}_{P_1^R} + \underbrace{\|v_1^I - r_{1,1}x_1^I\|^2}_{P_1^I} + \underbrace{\|v_2^R - r_{2,2}x_4^R\|^2}_{P_2^R} + \underbrace{\|v_2^I - r_{2,2}x_4^I\|^2}_{P_2^I}}^{P_{1,2}} + \underbrace{\|z_3 - r_{3,3}x_2\|^2}_{P_3} + \underbrace{\|z_4 - r_{4,4}x_3\|^2}_{P_4}. \tag{38}$$

Thus, as illustrated in Figure 1, (38) shows that the total cost of a leaf node $\mathbf{x}$ decomposes into the sum of three branch metrics, where P_4, P_3 and $P_{1,2}$ denotes the branch metrics for a branch at the first, second and third level of the tree, respectively.

The fact that $r_{3,4} = 0$ leads to a significant reduction in the complexity of the Schnorr-Euchner sorting for the first two stages of the tree. Specifically, the fact that $\mathbf{D}$ is diagonal implies that there is no interference or dependence between the symbols x_2 and x_3. Therefore, we can perform a single sort for the symbol x_3 emanating from the root, and *simultaneously* a single sort for the symbol x_2 emanating from its children.

The pseudocode of an efficient implementation of the proposed asymmetric golden code ML detector is shown in Figure 2. The first five lines represent initializations. In particular, the first two lines are a QR decomposition of the permuted effective channel

matrix in (23) and the computation of $\mathbf{z}$. The squared sphere radius $\hat{P}$, which represents the smallest cost (32) encountered so far, is initialized to infinity to ensure ML decoding (line 3). Sorting or Schnorr-Euchner enumeration is used for faster convergence. Only two sorting operations (line 4 and line 5) are required. In the pseudocode, the complex QAM alphabet $\mathcal{A}$ is represented by an ordered list, so that $\mathcal{A}(k)$ indexes the k-th symbol in the list. We next describe the remainder of algorithm, which can be interpreted as a two-level complex sphere decoder to choose the symbol pair $\mathbf{d} = [x_2, x_3]^\top$, followed by four independent slicers that separately decode x_1^R, x_4^R, x_1^I and x_4^I.

```
1  [Q, R] = QR decomposition(H_Π)
2  z = Q*y
3  P̂ = ∞
4  [P_4, Π_4] = sort_{a∈A}(|z_4 − r_{4,4}a|^2)
5  [P_3, Π_3] = sort_{a∈A}(|z_3 − r_{3,3}a|^2)
6  for k from 1 to q do
7      if(P_4(k) > P̂), break, end
8      for l from 1 to q do
9          if((P_3(l) + P_4(k)) > P̂), break, end
10         x_3 = A(k), x_2 = A(l)
11         v_1 = z_1 − r_{1,3}x_2 − r_{1,4}x_3, v_2 = z_2 − r_{2,3}x_2 − r_{2,4}x_2
12         x_1^R = Q(v_1^R/r_{1,1}), x_1^I = Q(v_1^I/r_{1,1})
13         x_4^R = Q(v_2^R/r_{2,2}), x_4^I = Q(v_2^I/r_{2,2})
14         P_1^R = |v_1^R − r_{1,1}x_1^R|^2, P_1^I = |v_1^I − r_{1,1}x_1^I|^2
15         P_2^R = |v_2^R − r_{2,2}x_4^R|^2, P_2^I = |v_2^I − r_{2,2}x_4^I|^2
16         P = P_1^R + P_1^I + P_2^R + P_2^I + P_3(l) + P_4(k)
17         if P < P̂ then
18             P̂ = P, x̂ = [x_1, x_2, x_3, x_4]
19         end
20     end
21 end
```

Fig. 2 Pseudocode of a fast ML decoder for the asymmetric golden code in quasistatic fading.

The two-level complex sphere decoder incorporates two common optimizations: radius update (line 18) and pruning (line 7, line 9). While these optimizations do not affect the worst-case complexity, they affect the average complexity significantly. The first level of the complex sphere decoder considers candidate symbols x_3 in ascending order of their branch metric P_4 (line 6). The second level of the complex sphere decoder considers candidate symbols x_2 in ascending order of their branch metric P_3 (line 8). The decoder then removes the interference caused by $\mathbf{d} = [x_2, x_3]^\top$ and forms the two intermediate variables v_1 and v_2 of (36), which are functions of the symbols x_1 and x_4 only (line 11).

Following the two-level complex sphere decoder and interference cancellation, the decoder decides on the remaining four PAM symbols x_1^R, x_4^R, x_1^I and x_4^I separately using independent slicers (lines 12 and 13). The corresponding branch metrics are calcualted in lines 14 and 15. The overall cost P for the current candidate symbol vector is updated in line 16. Radius update and best candidate vector update (line 18) occur if the current cost P is less than the previous smallest cost $\hat{P}$ in line 17.

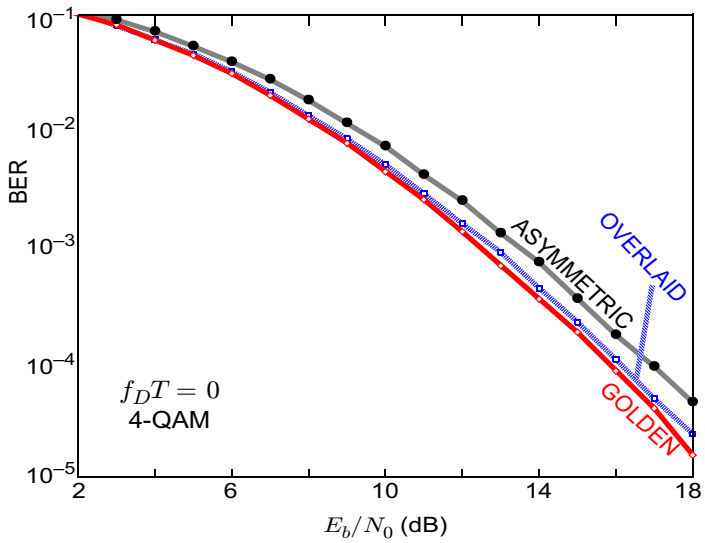

Fig. 3 Performance comparison for the two-input two-output channel.

5 Numerical Results

In this section, we compare the bit-error rate (BER) performance of the asymmetric golden code with the golden code and overlaid Alamouti codes of [10][11]. To avoid clutter we do not include the overlaid Alamouti code of [12] in our comparison; we simply note that it performs 0.1 dB worse than the overlaid Alamouti codes of [10][11].

In Figure 3, we show simulation results for quasistatic fading with ML detection implemented using the sphere decoder algorithm, assuming 4-QAM. The asymmetric golden code, which has the lowest decoding complexity under any channel condition, suffers a performance loss of 1.0 dB compared to the golden code. This is due to a reduction in the coding gain. The overlaid Alamouti codes also suffer a slight performance loss of 0.3 dB, which may also be attributed to a reduced coding gain.

In Figure 4, we illustrate the impact of a time-varying channel on the performance and complexity of the overlaid Alamouti and asymmetric golden code, assuming 64-QAM. The time-selectivity is quantified by f_DT, the maximum Doppler frequency normalized by the symbol period. The number adjacent to each point represents the corresponding value of f_DT. The case of quasistatic fading corresponds to $f_DT = 0$. For each space-time code, we plot a trajectory of "performance" versus "complexity" as the Doppler increases, where performance is quantified by the average SNR required to achieve BER $= 10^{-3}$, and where complexity is quantified by the average number of nodes visited by a complex sphere decoder that uses Schnorr-Euchner enumeration, sphere radius update and depth-first tree search. There are three trajectories:

– The left-most trajectory (labeled "overlaid + ignore") shows how the performance of the overlaid Alamouti codes of [10][11] degrades as the Doppler increases, when the receiver ignores the time variation and pretends that the channel is quasistatic. Such a strategy is ML for the special case of zero Doppler, and it is effective for slowly varying channels, but it quickly degrades as the Doppler frequency grows.

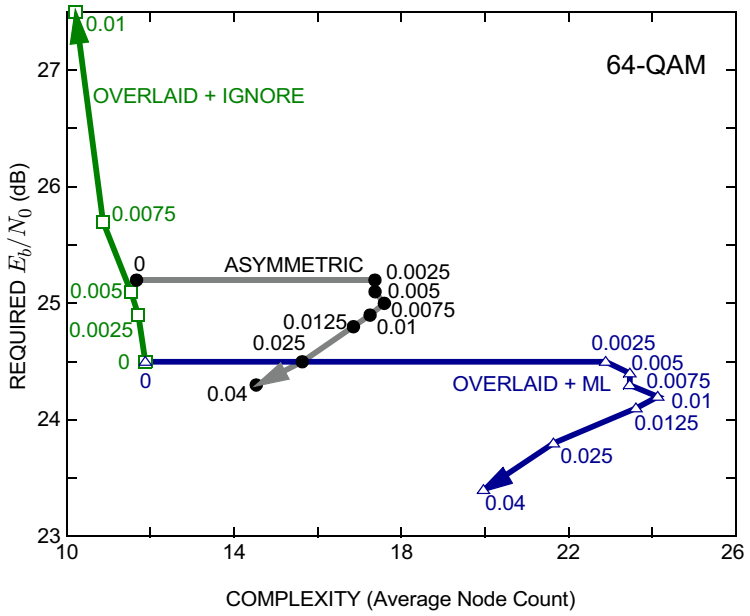

Fig. 4 Complexity and performance as a function of normalized Doppler $f_D T$.

- The right-most trajectory (labeled "overlaid + ML") shows the performance and complexity of the overlaid Alamouti codes of [10][11] with an ML detector that accounts for the time variations of the channel; the performance is good for all Doppler values but the complexity is high.
- The remaining trajectory (labeled "asymmetric") shows the performance and complexity of the asymmetric golden code with ML decoding. This trajectory is the only one of the three that starts in the desirable lower-left corner of the performance-complexity plane, and stays there for all values of the normalized Doppler frequency.

6 Conclusions

We introduced the asymmetric golden code, which asymmetrically scales the two layers of the golden code before adding. Furthermore, we proposed a fast ML decoding algorithm for the asymmetric golden code based on a unique tree construction that exploits the special structure of the effective channel matrix. The asymmetric golden code not only achieves the diversity-multiplexing tradeoff, but it maintains a low decoding complexity in both quasistatic fading and rapid time-varying fading channels.

A Optimal Asymmetry Coefficient $\mathcal{K}$

Since we are maximizing the coding gain for QAM alphabet, which is a subset of $\mathbb{Z}[i] \triangleq \{a+bi\}$, $a, b \in \mathbb{Z}$, where $i = \sqrt{-1}$, and because the asymmetric golden code is linear, the asymptotic coding gain of (3) can be written as:

$$\Gamma(\mathcal{K}) = \min_{(\Delta x_1, \Delta x_2, \Delta x_3, \Delta x_4) \in \mathcal{M}} |\det(\mathbf{C})|, \tag{39}$$

where $\mathcal{M} \triangleq \{\mathbb{Z} + i\mathbb{Z}\}^4 - \{0,0,0,0\}$ is the 4-tuple of all possible complex integers excluding $\{\Delta x_1, \Delta x_2, \Delta x_3, \Delta x_4\} = \{0,0,0,0\}$, which is the all zero 4-tuple. Since the difference between two integers is again an integer, we simplify the coding gain expression as follows

$$\Gamma(\mathcal{K}) = \min_{(x_1,x_2,x_3,x_4)\in\mathcal{M}} |\det(\mathbf{C})|. \tag{40}$$

Substituting the definition of $\mathbf{C}$ in (16) into (40) yields:

$$\begin{aligned}\Gamma(\mathcal{K}) &= \min_{(x_1,x_2,x_3,x_4)\in\mathcal{M}} \left| \frac{2}{1+\mathcal{K}^2}(u_1u_2^* - \mathcal{K}^2 u_3 u_4^*) \right| \\ &= \frac{1}{\sqrt{5}} \min_{(x_1,x_2,x_3,x_4)\in\mathcal{M}} \left| \frac{2}{1+\mathcal{K}^2} \left(g(x_1,x_2) - \mathcal{K}^2 g(x_3,x_4)\right) \right|, \end{aligned} \tag{41}$$

where

$$g(a,b) = \left(-|a|^2 + |b|^2 + \Re\{a^*b\} + i\cdot\sqrt{5}\Im\{a^*b\}\right). \tag{42}$$

We next find the value of $\mathcal{K}$ that maximizes (41). We proceed in two steps: first, we establish the bound $\Gamma(\mathcal{K}) \le 1/\sqrt{20}$; then, we show that $\mathcal{K} = 1/\sqrt{3}$ achieves the bound with equality.

To establish the bound, let us introduce $\mathcal{L} \subseteq \{(0,0,1,0),(1,0,1,0),(1,0,1+i,0)\} \subseteq \mathcal{M}$. Because $\mathcal{L}$ is a subset of $\mathcal{M}$, it clearly follows that $\min_{\mathcal{M}}\{\cdot\} \le \min_{\mathcal{L}}\{\cdot\}$, so that the coding gain of (41) can be bounded by:

$$\begin{aligned}\Gamma(\mathcal{K}) &\le \frac{1}{\sqrt{5}} \min_{(x_1,x_2,x_3,x_4)\in\mathcal{L}} \left| \frac{2}{1+\mathcal{K}^2} \left(g(x_1,x_2) - \mathcal{K}^2 g(x_3,x_4)\right) \right| \\ &= \frac{1}{\sqrt{5}} \min\left\{ \frac{2}{1+\mathcal{K}^2}\mathcal{K}^2, \frac{2}{1+\mathcal{K}^2}\left(1-\mathcal{K}^2\right), \frac{2}{1+\mathcal{K}^2}\left|1-2\mathcal{K}^2\right| \right\} \\ &\le \frac{2}{\sqrt{5}} \max_{1>\mathcal{K}>0} \min\left\{ \frac{\mathcal{K}^2}{1+\mathcal{K}^2}, \frac{1-\mathcal{K}^2}{1+\mathcal{K}^2}, \frac{\left|1-2\mathcal{K}^2\right|}{1+\mathcal{K}^2} \right\} \qquad (43) \\ &= \frac{1}{2\sqrt{5}} = \frac{1}{\sqrt{20}}. \qquad (44)\end{aligned}$$

The inequality of (43) follows from the fact that $h(\mathcal{K}) \le \max_{1>\mathcal{K}>0}\{h(\mathcal{K})\}$ for any function $h(\mathcal{K})$ and for any $\mathcal{K} > 0$. The equality in (44) is a result from the following lemma.

Lemma 3 *The maximum of the minimum is:*

$$\max_{1>\mathcal{K}>0} \min\left\{ \frac{\mathcal{K}^2}{1+\mathcal{K}^2}, \frac{1-\mathcal{K}^2}{1+\mathcal{K}^2}, \frac{\left|1-2\mathcal{K}^2\right|}{1+\mathcal{K}^2} \right\} = \frac{1}{4}, \tag{45}$$

and is acheived for $\mathcal{K} = 1/\sqrt{3}$.

Proof The functions $\mathcal{K}^2/(1+\mathcal{K}^2)$ and $(1-\mathcal{K}^2)/(1+\mathcal{K}^2)$ are monotonically increasing and decreasing, respectively. The function $|1-2\mathcal{K}^2|/(1+\mathcal{K}^2)$ is decreasing for $\mathcal{K} \in \left(0, 1/\sqrt{2}\right]$ and increasing for $\mathcal{K} \in (1/\sqrt{2}, 1)$. We find the maximum of the minimum over two regions; $\mathcal{K} \in \left(0, 1/\sqrt{2}\right]$ and $\mathcal{K} \in (1/\sqrt{2}, 1)$.

For $\mathcal{K} \in \left(0, 1/\sqrt{2}\right]$, the maximum of the minimum of (45) occurs at the intersection of the increasing function $\mathcal{K}^2/(1+\mathcal{K}^2)$ and the smaller of the two decreasing functions $(1-\mathcal{K}^2)/(1+\mathcal{K}^2)$ and $|1-2\mathcal{K}^2|/(1+\mathcal{K}^2)$. Since $|1-2\mathcal{K}^2| < (1-\mathcal{K}^2)$ for $\mathcal{K} \in \left(0, 1/\sqrt{2}\right]$, the maximum of the minimum occurs at the intersection of $\mathcal{K}^2/(1+\mathcal{K}^2)$ and $|1-2\mathcal{K}^2|/(1+\mathcal{K}^2)$, namely at $\mathcal{K} = 1/\sqrt{3}$. The maximum of the minimum is given by $\frac{1}{4}$.

For $\mathcal{K} \in (1/\sqrt{2}, 1)$, the maximum of the minimum occurs at the intersection of the decreasing function $(1-\mathcal{K}^2)/(1+\mathcal{K}^2)$ and the smaller of the two increasing functions $\mathcal{K}^2/(1+\mathcal{K}^2)$ and $|1-2\mathcal{K}^2|/(1+\mathcal{K}^2)$. Since $|1-2\mathcal{K}^2| < \mathcal{K}^2$ for $\mathcal{K} \in (1/\sqrt{2}, 1)$, the maximum of the minimum occurs at the intersection of $|1-2\mathcal{K}^2|$ and $(1-\mathcal{K}^2)$, namely at $\mathcal{K} = \sqrt{2/3}$. The maximum of the minimum is given by $1/5$. Therefore, the maximum of the minimum is $\frac{1}{4}$ and occurs at $\mathcal{K} = 1/\sqrt{3}$. □

We next show that the bound $\Gamma(\mathcal{K}) \leq \frac{1}{2\sqrt{5}}$ of (44) is in fact achievable with equality with $\mathcal{K} = 1/\sqrt{3}$. Substituting $\mathcal{K} = 1/\sqrt{3}$ into (41), we have:

$$\Gamma(1/\sqrt{3}) = \frac{1}{2\sqrt{5}} \min_{(x_1,x_2,x_3,x_4)\in\mathcal{M}} |3g(x_1,x_2) - g(x_3,x_4)| . \tag{46}$$

In order to show that $\Gamma(1/\sqrt{3}) = \frac{1}{2\sqrt{5}}$, we first prove that $\Gamma(1/\sqrt{3}) = 0$ only if $x_1 = x_2 = x_3 = x_4 = 0$ in the following lemma.

Lemma 4 *The function $f(x_1,x_2,x_3,x_4) = 3g(x_1,x_2) - g(x_3,x_4) = 0$, for $x_i \in \{\mathbb{Z}+i\mathbb{Z}\}$, $i \in \{1,2,3,4\}$, only if $x_1 = x_2 = x_3 = x_4 = 0$.*

Proof Assume that $f(x_1,x_2,x_3,x_4) = 0$, then we have that

$$3g(x_1,x_2) - g(x_3,x_4) = 0. \tag{47}$$

The equation in (47) implies that 3 divides $g(x_3,x_4)$, which is denoted $3|g(x_3,x_4)$. We next show that if $3|g(a,b)$, then $3|a$, $3|b$ and $9|g(a,b)$.

Let $a = 3l_a + r_a$ and $b = 3l_b + r_b$, where $l_a, l_b \in \{\mathbb{Z}+i\mathbb{Z}\}$, and $r_a, r_b \in \{0,1,2\}+i\{0,1,2\}$. Since, $3|g(a,b)$, we have that $3|g(r_a,r_b)$. By considering the finite number of possibilities for r_a and r_b, we can easily verify that $3|g(r_a,r_b)$ only if $r_a = r_b = 0$. Therefore, $3|a$ and $3|b$. Consequently, $g(a,b)$ is then given by

$$\begin{aligned} g(a,b) &= \left(-|3l_a|^2 + |3l_b|^2 + \Re\{3l_a^* 3l_b\} + i\cdot\sqrt{5}\Im\{3l_a^* 3l_b\}\right) \\ &= 9\left(-|l_a|^2 + |l_b|^2 + \Re\{l_a^* l_b\} + i\cdot\sqrt{5}\Im\{l_a^* l_b\}\right). \end{aligned} \tag{48}$$

As a result, we also have that $9|g(a,b)$.

Therefore, $f(x_1,x_2,x_3,x_4) = 0$ implies that $3|g(x_3,x_4)$, which in turn implies that $3|x_3$, $3|x_4$, and $9|g(x_3,x_4)$. However, $9|g(x_3,x_4)$ implies that $3|g(x_1,x_2)$, which in turn implies that $3|x_1$, $3|x_2$, and $9|g(x_1,x_2)$. We then have that $3|x_k$, $k \in \{1,2,3,4\}$. Hence, we can divide (47) by 3 and obtain an identical equation in the coefficients $y_k = \frac{x_k}{3}$, where $y_k \in \{\mathbb{Z}+i\mathbb{Z}\}$. Since we can repeat this argument and divide by 3 indefinitely, the only possible solution to $f(x_1,x_2,x_3,x_4) = 0$ is when $x_1 = x_2 = x_3 = x_4 = 0$. □

The desired result that $\Gamma(1/\sqrt{3}) = \frac{1}{2\sqrt{5}}$ follows from (46) and Lemma 4. In particular, Lemma 4 proves that $|3g(x_1,x_2) - g(x_3,x_4)| \neq 0$ for $(x_1,x_2,x_3,x_4) \in \mathcal{M}$. Since the real part of $3g(x_1,x_2) - g(x_3,x_4)$ is an integer, while the imaginary part is an integer multiple of $\sqrt{5}$, it follows immediately that:

$$\min_{(x_1,x_2,x_3,x_4)\in\mathcal{M}} |3g(x_1,x_2) - g(x_3,x_4)| = 1. \tag{49}$$

Substituting (49) into (46), we obtain that $\Gamma(1/\sqrt{3}) = \frac{1}{2\sqrt{5}}$. □

B Proof of the Key Property for Fast Decoding of the Asymmetric Golden Code on Quasistatic Fading Channel

Direct computation of the elements of $\mathbf{R}$ from the effective channel matrix in (23) yields:

$$\begin{aligned} r_{1,1} &= \sqrt{\frac{3}{2}}\sqrt{c^2\mu_1 + s^2\mu_2}, \quad r_{1,2} = 0, \quad r_{1,3} = \frac{3}{2\sqrt{5}r_{1,1}}(\mu_1 - \mu_2), \quad r_{1,4} = \frac{\sqrt{3}}{2r_{1,1}}\mu_3 \\ r_{2,2} &= \frac{1}{\sqrt{3}}\, r_{1,1}, \quad r_{2,3} = \sqrt{3}\, r_{1,4}^*, \quad r_{2,4} = \frac{-1}{\sqrt{3}}\, r_{1,3} \\ r_{3,3} &= \frac{\sqrt{27}|\mu_4|}{\sqrt{8}r_{1,1}^2}\sqrt{c^2\mu_1 + s^2\mu_2}, \quad r_{3,4} = 0 \\ r_{4,4} &= \frac{1}{\sqrt{3}}\, r_{3,3}, \end{aligned} \tag{50}$$

where these results are expressed in terms of the following four intermediate variables:

$$\begin{aligned}\mu_1 &= |h_{1,1}|^2 + |h_{1,2}|^2 \\ \mu_2 &= |h_{2,1}|^2 + |h_{2,2}|^2 \\ \mu_3 &= h_{1,1}^* h_{2,1} + h_{1,2}^* h_{2,2} \\ \mu_4 &= h_{1,1} h_{2,2} - h_{1,2} h_{2,1}. \end{aligned} \tag{51}$$

Because fading is quasistatic, we dropped the time index for simplicity of notation. Because $r_{1,2} = r_{3,4} = 0$, the matrices $\mathbf{A}$ and $\mathbf{D}$ in (24) are diagonal with real entires. □

References

1. IEEE 802.16e-2005: IEEE Standard for Local and Metropolitan Area Networks Part 16: Air Interface for Fixed and Mobile Broadband Wireless Access Systems Amendment 2: Physical Layer and Medium Access Control Layers for Combined Fixed and Mobile Operation in Licensed Bands, Feb. 2006.
2. S. M. Alamouti, "A Simple Transmit Diversity Technique For Wireless Communications," *IEEE J. Sel. Areas Commun.*, vol. 16, pp. 1451-1458, Oct. 1998.
3. V. Tarokh, N. Seshadri, and A. R. Calderbank, "Space-Time Codes for High Data Rate Wireless Communication: Performance Criterion and Code Construction," *IEEE Trans. Inf. Theory*, vol. 44, pp. 744-765, Mar. 1998.
4. P. W. Wolniansky, G. J. Foschini, G. D. Golden, and R. A. Valenzuela, "V-BLAST: An Architecture For Realizing Very High Data Rates Over The Rich Scattering Wireless Channel," *ISSSE* 98, pp. 295-300, 1998.
5. L. Zheng and D. Tse, "Diversity and Multiplexing: A Fundamental Tradeoff in Multiple Antenna Channels," *IEEE Trans. on Inf. Theory*, vol. 49, no 4, pp. 1073-1096, May 2003.
6. H. Yao and G. W. Wornell, "Achieving the Full MIMO Diversity-Multiplexing Frontier with Rotation-Based Space-Time Codes," in *Proceedings Allerton Conf. Commun., Cont., and Computing*, (Illinois), Oct. 2003.
7. J.-C. Belfiore, G. Rekaya, and E. Viterbo, "The Golden Code: A 2×2 Full Rate Space-Time Code with Non Vanishing Determinants," *IEEE Trans. on Inf. Theory*, vol. 51, April 2005.
8. P. Dayal and M. K. Varanasi, "An Optimal Two Transmit Antenna Space-Time Code And Its Stacked Extensions," *IEEE Trans. on Inf. Theory*, vol. 51, pp. 4348–4355, Dec. 2005.
9. M. O. Sinnokrot and J. R. Barry, "Fast Maximum-Likelihood Decoding of the Golden Code," *IEEE Trans. on Wireless Comm.*, accepted July 2009.
10. O. Tirkkonen and R. Kashaev, "Combined Information and Performance Optimization of Linear MIMO Modulations," in *Proc IEEE Int. Symp. Inf. Theory (ISIT 2002)*, Lausanne, Switzerland, p. 76, June 2002.
11. J. Paredes, A. B. Gershman, and M. G. Alkhanari, "A New Full-Rate Full-Diversity Space-Time Block Code With Nonvanishing Determinant and Simplified Maximum-Likelihood Decoding," *IEEE Trans. on Signal Processing*, vol. 56, pp. 2461-2469, June 2008.
12. S. Sezginer and H. Sari, "Full-Rate Full-Diversity 2×2 Space-Time Codes for Reduced Decoding Complexity," *IEEE Commun. Letters*, vol. 11, no. 12, pp. 1-3, Dec. 2007.
13. E. Biglieri, Y. Hong, and E. Viterbo, "On Fast Decodable Space-Time Block Codes," *IEEE Trans. on Inf. Theory*, vol. 55, no. 2, pp. 524-530, Feb. 2009.
14. M. O. Damen, K. Abed-Meraim, and J.-C. Belfiore, "Diagonal Algebraic Space-Time Block Codes," *IEEE Trans. on Inf. Theory*, vol. 48, no. 3, pp. 628-636, Mar. 2002.